MEASURING TRANSVERSE RELAXATION IN MYOCARDIAL TISSUE WITH 3T MAGNETIC RESONANCE IMAGING

By

Jared Guthrie Cobb

Thesis

Submitted to the Faculty of the

Graduate School of Vanderbilt University

in partial fulfillment of the requirements

for the degree of

MASTER OF SCIENCE

in

Biomedical Engineering

May, 2008

Nashville, Tennessee

Approved:

Professor Cynthia B. Paschal

Professor John C. Gore

To my lovely wife, Cheryl,

and

To my improbably supportive friends and family

and

To my silly dog Violet

ACKNOWLEDGEMENTS

Having spent the past few years blissfully immersed in academia, a brief pause to report some results and acknowledge those who have helped pave the way for me is warranted. When I returned to Vanderbilt four years after receiving my undergraduate degree, I was humbled by the privilege afforded me to return. My course through school has been lined with many supporters voicing encouragements along the way, and I would like to take this brief opportunity to thank them.

First, as always, I must acknowledge my wife, Cheryl, for allowing her husband to spend time away from home in pursuit of his aspirations. Her patience and guidance were invaluable. I would like to thank my parents for both instilling in me an expectation of excellence, and for teaching me how to balance life at work and at home. Thanks also go to my brother, Evan, who undertook a similar journey a few years ago and has always inspired me with his good humor and *joie de vivre*.

Thanks go especially to my advisor, Dr. Cynthia Paschal, who very patiently listened to my explanation of concepts in a Melvillian flow of endless phrases, artfully punctuated, only to intercede with a single crystalline, yet equivalent, sentence. I wish to thank Dr. Brian Welch for his encyclopedic knowledge of all

things Philips, and also to Dr. Huairen Zeng for his help debugging my pulse programming code.

As for my classmates, I would like to acknowledge Mary Loveless and Rowena Ong for their friendship and camaraderie through the many hours of preliminary exam cramming. I would like to thank Robert E. Lee for teaching me the ability to extricate myself from the minutia of a problem to better my understanding of the whole picture. I also owe thanks to the other members of my lab, especially Paul J. Hilt, for his help with experiments and equipment week in and week out. And that leads me back to the rest of my classmates and colleagues, many of whom are represented here in the data as subjects. For the many hours they lay strapped to a table in a huge magnet, listening to me monotonously drone, “breathe in… breathe out… hold“, I am eternally grateful.

This research was graciously supported by Drs. Cynthia Paschal and John Gore. Funding was provided by the Vanderbilt University Department of Biomedical Engineering and the National Institutes of Health grant number R01-EB00214.

TABLE OF CONTENTS

Page:

LIST OF FIGURES

LIST OF TABLES

CHAPTER I

INTRODUCTION

Background and Significance

Coronary artery disease remains one of the most significant causes of death in western societies despite rapid advances in medical technology and interventional treatments over the last 25 years (1). These treatments have been guided in large part by advances in medical imaging modalities such as echocardiography, computed tomography (CT), positron emission tomography (PET), and magnetic resonance imaging (MRI).

MRI is a relatively new form of medical imaging relying on the application of electromagnetic principles to visualize anatomy and function. An external magnetic field can be used to generate a net magnetic moment in the sample to be imaged. Magnetic moments then align with that field and begin to precess about it. The angular frequency of precession scales linearly with the strength of the external field. Thus a stronger external field results in a faster precessional frequency. The interactions of nuclear magnetic moments may be harnessed for imaging purposes by clever application of magnetic field gradients and radiofrequency pulses. A spatially varying magnetic field applied across a tissue sample will cause the moments to precess at different rates. By exciting the sample with a series of

radiofrequency (RF) pulses, the spins may be pushed out of alignment with the external field, synchronized, or otherwise manipulated to produce an RF field that can be measured in a receiving coil. This received signal may then be digitally processed by Fourier transform to produce an image (2).

Image contrast in MRI is governed by the complex interactions of magnetization and tissue composition and structure. MRI systems can be used to measure the time constants that characterize these interactions in different tissue types and conditions. Recently developed high-field magnets, gradient systems, and coil technologies allow MRI to be used as a sophisticated diagnostic tool in a variety of clinical applications. Of particular interest is the ability to use MRI to non-invasively probe cardiac tissue for myocardial infarction (MI) as a result of ischemia, to assess candidacy for reperfusion therapy, and to identify responses to stress agents.

Two MRI methods have become viable alternatives to PET or SPECT for determining ischemia in myocardial tissue (3, 4). The first technique is generally referred to as delayed gadolinium (Gd) contrast hyperenhancement whereby several minutes after contrast injection, infarcted myocardium exhibits image enhancement due to gadolinium chelate accumulation (5-8). The second technique is blood oxygen level dependence (BOLD) imaging. This method relies on an endogenous source of contrast, the oxygen level dependence of the myocardial signal. The effects of local changes in tissue oxygenation in the

myocardial microvasculature are manifested in altered transverse relaxation rates (T2 and T2*) (9-12). For ischemic or infarcted tissue, the lack of adequate perfusion is evident in lower measured transverse relaxation rates as compared to regions of adequate oxygen supply (11, 13). Transverse relaxation variations due to normal perfusion gradients in these tissues have not been reported.

Since the advent of clinical 3T MRI, the inherent signal to noise advantage has been much publicized as driving the future of clinical cardiac care (5,8). However, increased SAR restrictions, susceptibility artifacts, and standing waves pose challenges not apparent at 1.5T. Much effort has been expended developing phased array coils, new sequence techniques, navigator gating, and other methods to mitigate the disadvantages of thoracic imaging at 3T. Most clinical imaging utilizes delayed contrast enhancement and SSFP cine techniques to confirm the functional status of the heart (6,8). However, these sequences are not directly applicable to measuring the myocardial BOLD effect. Applying the knowledge gained improving clinical high-field imaging towards improving myocardial BOLD imaging has not been reported.

Several measurement approaches have been previously taken to measure BOLD effects in myocardium including gradient-echo (GRE) (9-11), spin-echo (SE) (14,15), and steady-state free precession (SSFP) based imaging techniques (13,16). Each approach attempts to maximize T2 or T2* BOLD contrast at a given

field strength while minimizing inherent disadvantages each technique carries with respect to artifacts and noise.

Specific Aims

The goal of the present work was to develop methods that overcome the practical difficulties of 3T human myocardial imaging and to determine reliable reference values for transverse relaxation times across normal human myocardium. It is of note that the typical protocol provided by the major MRI manufacturers for transverse relaxation mapping is a single 2-echo scan for *in vivo* measurement. Given only two data points to define an exponential decay, these 2-echo protocols may not allow for reliable measurements (17,18). With the goal of reliably measuring transverse relaxation for use in myocardial imaging, the following specific aims were developed.

1. To test a series of multi-echo, breath-hold scans for the measurement of T2 and T2* at 3 Tesla.
2. To optimize T2 and T2* methods with sufficient resolution to distinguish endo- and epicardium.
3. To evaluate the accuracy and repeatability of these methods.

Achievement of these aims will enable reliable detection of subtle changes in tissue properties with good spatial resolution at high field, yielding new insight into basic questions about cardiac physiology.

CHAPTER II

MEASURING TRANSVERSE RELAXATION IN MYOCARDIAL TISSUE WITH 3T MAGNETIC RESONANCE IMAGING

Introduction

Coronary artery disease remains one of the most significant causes of death in western societies despite rapid advances in medical technology and interventional treatments over the last 25 years (1). These treatments have been guided in large part by advances in medical imaging modalities such as echocardiography, computed tomography (CT), positron emission tomography (PET), and magnetic resonance imaging (MRI) that allow physicians to gather important information about cardiac function and disease state.

Of particular interest is the ability to use MRI to non-invasively probe cardiac tissue for myocardial infarction (MI) as a result of ischemia, to assess candidacy for reperfusion therapy, and to identify responses to stress agents. Currently PET and single photon emission tomography (SPECT) are advocated for these purposes; however each technique is limited by a relatively low spatial resolution as compared to MRI and carries a dose of ionizing radiation (3, 19).

Two MRI methods have become viable alternatives for determining ischemia in myocardial tissue (3,4). The first technique is generally referred to as delayed gadolinium (Gd) contrast hyperenhancement whereby several minutes after contrast injection, infarcted myocardium exhibits image enhancement due to gadolinium chelate accumulation (5-8). However, for patients with renal dysfunction, Gd is contraindicated due to the risk of nephrogenic systemic fibrosis (NSF) (20,21). In this case it would be advantageous to have an equivalent, non-invasive test. Blood oxygen level dependence (BOLD) imaging fulfils this need by taking advantage of an endogenous source of contrast, the oxygen level dependence of the myocardial signal. The effects of local changes in tissue oxygenation in the myocardial microvasculature are manifest in altered transverse relaxation rates (T2 and T2*) (9-12). For ischemic or infarcted tissue, the lack of adequate perfusion is evident in lower measured signal as compared to regions of adequate oxygen supply (11,13). Transmural variations across the myocardium have been well characterized at 1.5 and 3T using first-pass T1-weighted imaging. These studies show regions of hypoperfusion in the free-wall endocardium due to increased contractile forces and to the smaller diameter of the feeding vessels (22, 23). Transverse relaxation variations due to normal perfusion gradients in these tissues have not been reported. However preliminary studies have been done in infarcted tissue demonstrating the effects of reduced perfusion on transverse relaxation in ischemic tissue (11).

Several measurement approaches have been published reporting these BOLD effects in myocardium including: gradient-echo (GRE) (9-11), spin-echo (SE) (14,15), and steady-state free precession (SSFP) based imaging techniques (13,16). Each approach attempts to maximize T2 or T2* BOLD contrast at a given field strength while minimizing inherent disadvantages each technique carries with respect to artifacts and noise.

The gradient-echo based approach to measure the myocardial BOLD effect was initially adapted from brain and skeletal muscle imaging protocols and has been demonstrated *in vivo* and *ex vivo* research at a variety of field strengths (10,24). Using increasingly available clinical 3T magnets, GRE techniques suffer susceptibility artifacts at the heart-lung interface and at the posterior vein of the left ventricle (PVLV) (25,26). Spin-echo based approaches have generated some interest as they are relatively immune to this problem, but feature a limited potential for BOLD contrast and a slower rate of signal acquisition as compared to T2* measurement techniques (16,25,27). Cardiac imaging with SSFP techniques has recently become feasible due to advances in gradient performance (13,16,28). The BOLD effect, as measured via T2-prepped SSFP, is determined by a combination of proton density weighting, T1, and T2 effects. SSFP offers good SNR and blood-myocardium contrast, but it is difficult to achieve control over T1 effects and other artifacts at high field (13,29).

Since the advent of clinical 3T MRI, the inherent signal to noise advantage has been much publicized as driving the future of clinical cardiac care (5,8). However, increased SAR restrictions, susceptibility artifacts, and standing waves pose challenges not readily apparent at 1.5T. Much effort has been expended developing phased array coils, new sequence techniques, navigator gating, and other methods to mitigate the disadvantages of thoracic imaging at 3T. Most clinical imaging utilizes delayed contrast enhancement and SSFP cine techniques to confirm the functional status of the heart (6,8). However, these sequences are not directly applicable to measuring the myocardial BOLD effect. Applying the knowledge gained improving clinical high-field imaging towards improving myocardial BOLD imaging has not been reported.

The goal of the present work was to develop methods that overcome the practical difficulties of 3T human myocardial BOLD imaging and to determine reliable reference values for transverse relaxation times across normal human myocardium. It is of note that the typical protocol provided by the major MRI manufacturers for transverse relaxation mapping is a single 2-echo scan for *in vivo* measurement. Given only two data points to define an exponential decay, these 2-echo protocols may not allow for reliable measurement of transverse relaxation (17,18). With the goal of reliably measuring transverse relaxation for use in myocardial BOLD imaging, a series of multi-echo, breath-hold scans were tested to optimize the measurement of T2 and T2* at 3 Tesla with resolution sufficient enough to distinguish endo- and epicardium. Accurate measurement of T2 and T2*

with these new techniques at high field will allow researchers to consistently detect subtle changes in tissue properties, yielding new insight into basic questions about cardiac physiology.

Methods

Nine healthy volunteers were recruited to investigate magnetic resonance tissue properties of normal myocardium. The average age for the six male and three female volunteers was 24.8 ± 1.6 years. Volunteers underwent safety screening and provided written informed consent to participate in the study. The local Institutional Review Board (IRB) approved the study protocol. Subjects were imaged in the supine position using a 3.0T MRI scanner with a six-channel cardiac imaging coil (Philips Achieva 3T, Philips Medical Systems, Best, NE).

The imaging protocol began with an anatomic localizer and reference scan for parallel imaging. Short-axis views were established using a real-time slice planning sequence. To make the most uniform static magnetic field over the tissues of interest, shim volumes were prescribed to include the entire LV in plane and extending one centimeter on both sides of the imaging plane. First and second order shimming was used. Then, a series of turbo spin-echo and turbo field-echo scans were conducted as described below. Common to all scans was the use of triggered acquisition to place the imaging window during late diastole. Also, black-blood double-inversion pre-pulses were used prior to each image acquisition to null signal from blood in the ventricles (14). To facilitate breath holding for slower

cardiac rates, most scans were limited to 15 cardiac cycles to keep the total scan time less than ~20 seconds. Subjects were instructed to hold their breath at a comfortable end expiratory position, functional reserve capacity (FRC), prior to the imaging session (30).

Turbo Spin-Echo

Three multi-echo turbo spin-echo (TSE) T2-measurement methods were tested. Each method involved tradeoffs between acquired data as measured by phase encoding (PE) lines per image versus number of echo-image sample points obtained along the T2 decay curve. The first method utilized an interleaved pair of standard dual-echo TSE scans (2x2-echo), where in each scan fourteen echoes from the echo train were encoded for two TSE images. With seven lines acquired per image per cardiac cycle, and 15 cardiac cycles, this method yielded a total of 105 phase encoding lines per image. Low spatial frequency phase encoding lines were acquired first (i.e., “low-high” profile order), and effective echo times were 20 and 60 ms for the first scan and 40 and 80 ms for the second scan. The same transmitter and receiver gains were used for each scan to eliminate arbitrary signal scaling. Further scan details are summarized in Table 1.

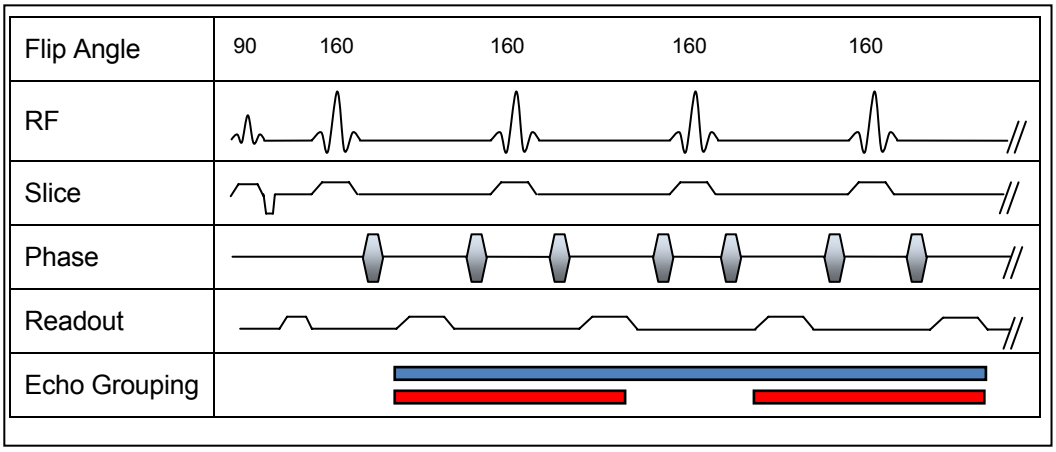

Figure 1: Sample ME TSE sequence. The blue bar at bottom indicates 4-echo grouping. Red bars indicate 8-echo grouping.

The second method investigated was a single, custom-designed TSE scan where 16 echoes from the echo train were encoded as four TSE images (4-echo TSE). Thus, the first four echoes were assigned to the first echo-image, the second set of four echoes to the second echo-image, and so on. With an inter-echo spacing of 6 ms and low-high profile order, this resulted in effective echo times of: 6, 30, 54, and 78 ms. See Table 1 for details. An illustration of this echo train division is given in Figure 1.

The third method investigated was a single, custom-designed TSE scan where, similar to the 4-echo TSE method, 16 echoes from the echo train were encoded as eight TSE images (8-echo TSE). Thus, the first two acquired echoes are assigned to the first echo-image, and then the next two acquired echoes are assigned to the second echo-image, and so forth. With inter-echo spacing of 6 ms and a low-high profile order, this method resulted in echo times of: 6, 18, 30, 42, 54, 66, 78, and 90 ms. A summary of the features of each method are given in Table 1.

Parameters common to all TSE methods include: TR = 1 RR interval, FOV = 320 x 256 mm, matrix interpolation to 256 x 256, slice thickness = 6mm, excitation flip angle = 90°, refocusing flip angle = 160°, half-scan = 0.8, scan percent = 0.8 and parallel imaging (SENSE (31, 32)) reduction factor = 1.5.

Table 1: TSE Methods

TSE Method	*RO Points*	*TSE Factor*	*Shots (cardiac cycles)*	*PE Lines / Image*	*Pixel BW (Hz)*
2 x 2-echo	256	14	15 x 2	105	352
4-echo	256	16	15	60	294
8-echo	256	16	22	44	291

Turbo Field-Echo

Three multi-echo turbo field-echo (TFE) T2*-measurement methods were tested. These methods were designed to highlight the differences between achievable bandwidth per pixel and echo time constraints versus the number of sample points obtained along the T2* decay curve. Minimum bandwidth between pixels was desired to minimize the effects of electronic or thermal noise generated by the scanner (33). As the inter-echo spacing was decreased, the water-fat shift parameters (1/ pixel bandwidth) (2) had to be correspondingly reduced, resulting in larger pixel bandwidths as the number of acquired echoes increased. The first method used was a series of three dual-echo TFE sequences. The first echo was fixed at 2.3 ms and second echoes were set at 6.9, 11.5, and 18.4 ms, resulting in

a total of four unique time point samples along the T2* decay curve. The same transmitter and receiver gains were used for each scan. Minimum pixel bandwidth achievable was 294.3Hz/pixel. A four-echo TFE sequence was then used with the first echo set at 2.3 ms and subsequent echoes incremented, in-phase, up to 16.1 ms with a fixed ΔTE of 4.6 ms, resulting in four decay curve samples. Minimum pixel bandwidth was also scanner limited to 294.3Hz/pixel. This sequence is illustrated in Figure 2.

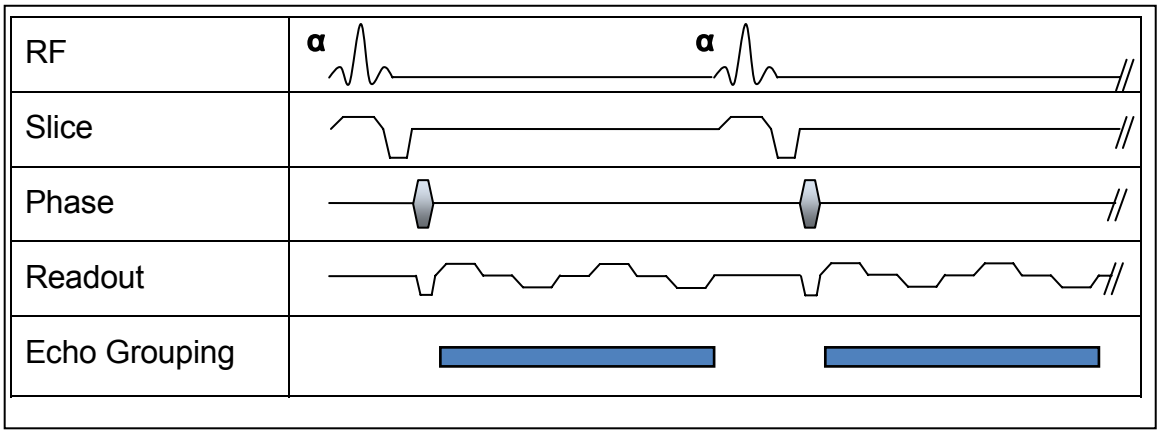

Figure 2: Sample 4-echo TFE sequence. Four echoes are acquired per alpha excitation. The blue region indicates the four acquired echo times.

The last method utilized an eight-echo TFE sequence with the first echo set at 2.3 ms and later echoes incremented, in-phase, up to 18.4 ms with a ΔTE of 2.3 ms, resulting in eight decay curve samples. Here the short ΔTE required the use of a minimum pixel bandwidth of 482.5Hz/pixel. A summary of these features is given in Table 2.

Table 2: TFE Methods

TFE Method	*RO Points*	*TFE Factor*	*Shots (cardiac cycles)*	*PE Lines / Image*	*Bandwidth/ Pixel*
3 x 2-echo	192	8	15 x 3	120	294
4-echo	192	8	15	120	294
8-echo	192	8	15	120	483

Common scan parameters for all TFE sequences include: FOV = 320 x 256 mm, acquired matrix = 192 x 120, interpolated to 256 x 256; Turbo factor = 8 (i.e. eight TR's per cardiac cycle), shots acquired = 15 (number of cardiac cycles), TR = 25 ms, flip angle = 25°, and slice thickness = 6 mm. Parallel imaging was not used for TFE scans.

Image Analysis

Average signal values were taken from regions of interest (ROIs) in the mid-ventricular septum to compute T2 and T2* by fitting the data to a monoexponential decay curve. An example ROI is given in Figure 3. Maps of T2 and T2* were also generated using custom software written in MATLAB R2007a using each pixel as an ROI (The MathWorks, Inc., Natick, MA). T2 and T2* values, signal-to-noise ratios (SNR), quality of data fit to decay curves, and acquired voxel sizes were assessed among

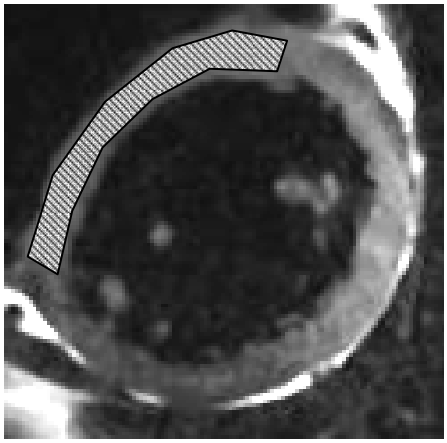

Figure 3: Mid-ventricular ROI on a 2E TSE Image. Conservative margins were used to minimize partial volume effects.

the different methods. SNR was calculated from the shortest echo-image by taking the mean signal in the ROI divided by the standard deviation of signal in an adjacent ROI of homogenous liver tissue. Background signal was not used for SNR calculations as there was limited clear background signal in the FOV and as it would underestimate the magnitude of measured noise (34). Liver signal was chosen as it is subjected to less apparent motion artifact and, unlike the heart, in the plane of interest does not carry a susceptibility boundary with the lung.

Additionally, endo- and epicardial ROIs were assessed in the free wall for signal differences that may be attributed to transmural perfusion gradients. The endocardial ROI was drawn from the inner wall of the LV to the midline of the ventricle, and the epicardial ROI was drawn from this line to the exterior wall of the LV. See Figure 4.

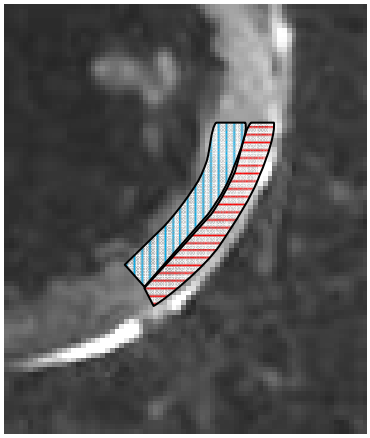

Figure 4: Endo- and epicardial ROIs. The red horizontal bars indicate the epicardial ROI. The blue vertical bars indicate the endocardial ROI.

Results

T2 for the ventricular septum was 59.5 ± 7.9 ms (N=9) across all methods and all subjects with R^2's averaging 0.976 for the monoexponential fits. A representative first-echo SE image is given in Figure 5a. A map of T2 created via the 2x2-echo method is given in Figure 5b.

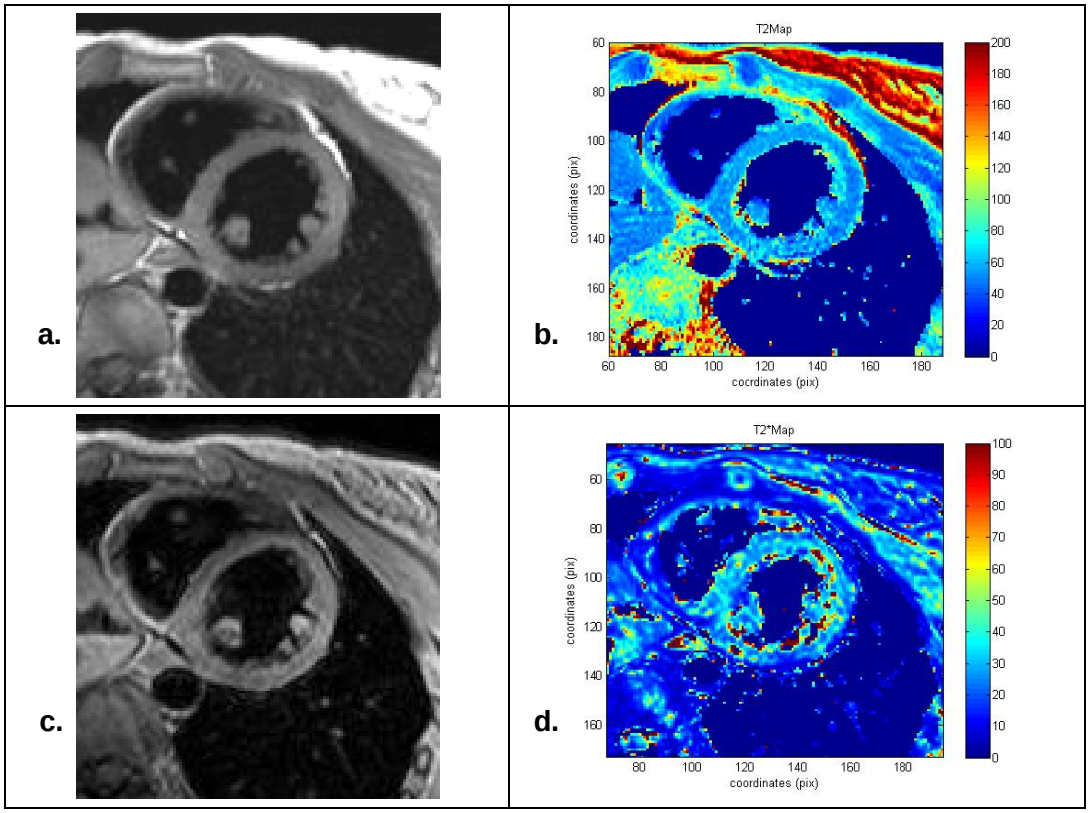

Figure 5: Representative images and maps. a. 2-echo TSE image, b. 2x2-echo T2 map, c. 4-echo TFE image, d. 4-echo T2* map. All images are from the same scan session and subject.

T2* for the ventricular septum was 31.6 ± 6.1 ms (N = 9) across all methods and across all subjects with R^2's averaging 0.929 for the monoexponential fits. A first echo TFE image is given in Figure 5c and a map is given in Figure 5d. Summaries of measured T2 and T2* values for each methodology are provided in Table 3 and Table 4, respectively.

One-way analysis of variance (ANOVA) revealed no statistical difference in reported standard deviations for the T2 values compared across subjects and correspondingly, a student's t-test comparing the T2 methods showed no statistical differences in the reported means (35). The 2x2-echo method of T2 measurement

provided the lowest variance of mean T2 values across subjects. The 4-echo method gave the best curve fits, with the highest reported R^2 average value of 0.983. The difference in quality of monoexponential curve fits between the 2x2- and 4-echo methods and the 4- and 8-echo methods were significant as compared using the student's t-test ($p = 0.0004$, $p = 0.023$ respectively). The R^2 values compared between the 2x2- and 8-echo methods were not considered significantly different. The highest average SNR reported for T2 measurement was given by the 8-echo method, however the differences in means and variances of SNR across all techniques were not significant. The 2x2-echo method gives the best acquired resolution as compared to the 4- and 8-echo methods.

One-way ANOVA revealed no statistical difference in reported standard deviations for mean T2* values compared across subjects and, a student's t-test comparing the TFE methods showed no statistical differences in the reported means. The 4-echo method of T2* measurement provided the smallest standard deviations of mean T2* values across subjects. The 4-echo method yielded the best curve fits, with the highest reported R^2 average value of 0.949. The differences in quality of monoexponential curve fits between the 3x2- vs. 4-echo and the 4-echo vs. the 8-echo methods were significant ($p = 0.007$ and $p = 0.043$ respectively). The R^2 values compared between the 3x2- and 8-echo methods were not considered significantly different. The highest average SNR reported for T2* measurement was given by the 8-echo method; however the differences in means and variances

of SNR across all techniques were not significantly different. All TFE methods resulted in the same acquired voxel size.

Endo- and epicardial ROIs showed a statistically significant difference in mean T2* ($p = 0.05$) with the endocardial T2* ROI being less than the epicardial T2* ROI. There was no significant difference in mean T2 measured across the myocardium. Whole LV analysis of T2 and T2* was prohibited by uncompensated susceptibility effects and other artifacts that appeared in varying regions from subject to subject in the free wall of the LV.

Table 3: TSE results across subjects in the mid-ventricular septum (N = 9).

TSE Method	*Average T2 (ms) across subjects*	*Stdev. of T2 (ms)*	*Avg. curve fit R^2*		*SNR in septum*
2x2-echo	57.6	9.1	0.971	*	10.6
4-echo	61.6	7.8	0.983	*	14.8
8-echo	58.5	7.0	0.971		15.0
Average across all methods	59.5	7.9	0.976		13.8

*p<0.05

Table 4: TFE results across subjects in the mid-ventricular septum (N = 9).

TFE Method	*Average T2* (ms) across subjects*	*Stdev. of T2* (ms)*	*Avg. curve fit R^2*		*SNR in septum*
3x2-echo	31.6	13.1	0.919	*	11.7
4-echo	31.2	9.6	0.949	*	11.6
8-echo	32.2	10.3	0.917		9.0
Average across all methods	31.6	6.1	0.929		10.1

*p<0.05

Discussion and Conclusions

Measured T2 values were very consistent both in reported means and in quality of fit across the three scan methods. This reveals that any of the scan methods may be used to generate consistent T2 values. However, it is certainly advantageous from the patient's perspective to use the 4- or 8-echo methods as they require only a single-breath hold. This study reports an average myocardial T2 at 3T of 59.5 ± 7.9 ms. Another recent *in vivo* report gives slightly shorter T2 values in the myocardium as 54 ± 5.7 ms (16). It is important to note that ideal echo spacing for monoexponential fits includes sample points on either side of the measured value with emphasis placed on acquiring early echoes (17,18,36). Echo spacing for each of the investigated methods was well spaced around the reported mean T2 value, and the 4- and 8-echo methods in particular resulted in many early TE samples as compared to the 2x2-echo method.

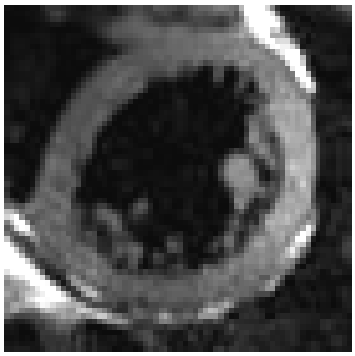

a. 2-E TSE

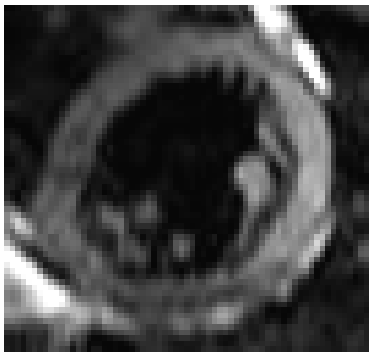

b. 4-E TSE

c. 8-E TSE

Figure 6: Representative TSE image series compared in a single subject.

Given the dramatic reduction in phase encoding lines for the 4- and 8-echo spin-echo-based measurements, an image quality reduction was expected as

compared to the 2x2-echo series. Even so, SNR increases slightly from the 2x2-, to 4-, to 8-echo methods. This is presumably due to differences in echo times along with the effects of increasing voxel size overwhelming the effects of phase encode line reduction. Thus, the reported SNR values may be considered only a general measure of image quality for loose comparison among methods.

Given that the typical in-plane resolution for the 2x2-echo method was 1.25x1.6 mm^2, this method resulted in the highest spatial resolution scans and thus gave the sharpest images. By sacrificing the number of phase encoding lines acquired for additional temporal sampling of the T2 decay curve, the 4- and 8-echo methods resulted in more elongated voxels, typically 1.25x3.2mm^2 and 1.25x4.6mm^2 respectively. Given this, partial volume effects became apparent as softened borders along tissue boundaries. See Figure 6 above.

Image artifacts were generally confined to the free wall of the left ventricle. It is hypothesized that a major source of image variation in this area was due to uncompensated susceptibility effects. These effects are presumably due to the use of 160° refocusing pulses instead of the 180° pulses typically prescribed in modified Carr-Purcell-Meiboom-Gill (CPMG) experiments (17). Imperfect refocusing of transverse magnetization at the long echo times measured here as compared to T2 may account for these susceptibility effects being more apparent than in the gradient-echo methods (36). Along with the susceptibility effects, other general sources of image artifacts are imperfect breath holding or cardiac motion

during the acquisition window. Given that the 4-echo method had similar image characteristics to the 8-echo, but allowed for higher resolution scans, demonstrated the best curve fits, and required only a single breath hold, the 4-echo method is recommended over the 8-echo method.

Measured T2* values were very consistent both in reported means and in SNR across the three scan methods. This reveals that any of the scan methods may be used to generate consistent T2* values. However it is worth noting that even with the similar SNR among the TFE series, significant decreases in the standard deviation of the T2* value and increases in the quality of fit (R^2) exist favoring the 4-echo method. It is also advantageous to acquire data in a single breath hold, shifting preference away from the 3x2-echo method. Given the above evidence the 4-echo method is recommended for measuring T2*.

The reported mean T2* value of 31.6 ± 6.1 ms is consistent with other published values. Recent research at 3T reports values for T2* *in vivo* as 27.3 ± 6.4ms (37) and 33.3 ± 2.7 ms (38). It is important to note that all TEs utilized in the TFE scans were shorter than the measured T2* values. Ideally TEs should be spaced on either side of the measured value, with emphasis placed on measuring early TEs (18). However, image degradation noted beyond the latest measured echo time (18.4 ms) was so severe at 3T as to preclude extending temporal sampling.

TFE images showed less variation in image quality as the number of echoes increased compared to the TSE series. This was expected due to the fact that all three TFE methods used the same number of phase encoding lines (see Table 2). Unlike in the TSE images, here the SNR results may be directly compared due to the images carrying the same first echo times. The TFE SNR was mainly expected to vary as a result of minimum achievable pixel bandwidth; however there was no significant difference measured in SNR across methods.

Image artifacts in the TFE scans were affected by the same physiologic noise seen in the TSE methods, including poor breath-hold motion suppression, cardiac motion during acquisition, in addition to susceptibility artifacts that are characteristic of gradient-echo based sequences. This phenomenon is observed especially at boundaries of tissue with large differences in magnetic susceptibility, such as at the heart-lung interface and around the posterior vein of the left ventricle (25) (26). These artifacts can be seen in the free wall of the left ventricle in Figure 7 above. Similar artifacts limited more comprehensive free wall and whole ventricle signal analysis.

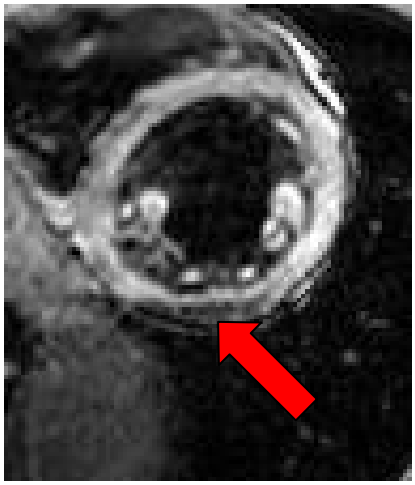

Figure 7: First echo image of a 2-echo TFE sequence. The arrow points to a susceptibility artifact at the heart-lung interface.

High resolution 4-echo scans were utilized to facilitate the measurement of potential endo- and epicardial signal gradients. The techniques described here yield voxel sizes well below other recent investigations at 3T (16,22,37). Endo- and epicardial ROIs were investigated for observed gradients due to differences in transmural myocardial perfusion. It is of particular note that the observed change in signal for T2* was in the opposite direction as predicted by previous theoretical (12) and oxygen-dependant studies (22,39). Much of that research focuses on observed changes as a result of myocardial infarction, not on any inherent T2* gradient that may exist as a result of perfusion differences. As the endocardium is more hypoxic than the epicardium (11), the relative T2* should theoretically be lower in the endocardial ROI than in the epicardial ROI. The mismatch between the theoretically predicted higher T2* values in the epicardium and our results measuring lower T2* values may be partially explained by increased susceptibility effects in the free wall. These effects may have suppressed signal in the epicardium at longer TEs to the extent that curve fits to the pixels in this area resulted in significantly lower T2* measurements than expected ($p = 0.04$). The results for T2 measurement in the free wall did not show a significant difference in measured endo- and epicardial ROIs; however the trend for lower epicardial signal did follow the GRE measurements. These findings reveal the potential difficulty in using GRE based techniques for visualizing BOLD gradients in the free wall of the myocardium at 3T.

Ideally, a very large number of echoes would be used to accurately characterize transverse relaxation *in vivo*. However, unlike in NMR experiments, there are many issues limiting the amount of echoes that may be practically acquired in cardiac MRI. Typically, clinical imaging attempts to maximize SNR, decrease voxel size, and limit specific absorption rate (SAR) exposure. This methodology shifts available SNR and acquisition time away from accurately measuring tissue characteristics towards visualization of detailed anatomy both statically and dynamically (6, 40). However, the importance of utilizing the increased temporal and SNR gains available with high-field magnets to more precisely characterize endogenous contrast mechanisms must not be minimized. The high quality of curve fits reported here reflects the accuracy of the measured transverse relaxation values. There is unfortunately no gold standard for *in vivo* cardiac tissue T2 or T2* measurement, therefore comparison to other published results in terms of reported means and variance may be the only general measure of accuracy. It is important to further investigate these techniques for use in cardiac research describing the myocardial BOLD effect, perfusion tests, and other aspects of oximetry.

This study was limited in part by the small number, relative youth, and health of the available volunteers. Two-echo methods were not investigated as they have been in wide use for estimating transverse relaxation for some time (10,14). Inherent in a 2-echo design is an overly simplistic two point fit to an exponential decay curve, and this would have precluded quality of curve fit comparison to the multi-echo

methods described here (17,18). The use of newly developed 3rd order shim tools that have been applied in SSFP imaging (28) should improve future results. It would also be of interest to investigate these techniques in combination with navigator gated acquisition, allowing for signal averaging over extended periods of time.

In conclusion, this work at 3T demonstrates the feasibility of multi-echo sampling of T2 and T2* while maintaining adequate SNR and voxel sizes to investigate endo- and epicardial gradients. Given the inherent advantage in multi-echo temporal sampling of transverse relaxation over 2-echo methods, utilizing these techniques will be of importance when describing subtle differences in tissue relaxation. As it is of continued importance to characterize myocardial oximetry non-invasively it is imperative to have the most accurate sequences available for this type of measurement. These results suggest that the 4-echo methods are best suited for optimal T2 and T2* sampling in the mid-ventricular septum. This work presents reliable, high spatial resolution techniques for measuring T2 and T2* and provides reference values for transverse relaxation times in the normal myocardium.

CHAPTER III

CONCLUSIONS AND FUTURE WORK

This work at 3T demonstrates the feasibility of multi-echo sampling of T2 and T2* while maintaining adequate SNR and voxel sizes to investigate endo- and epicardial gradients. Given the inherent advantage in multi-echo temporal sampling of transverse relaxation over 2-echo methods, utilizing these techniques will be of importance when describing subtle differences in tissue relaxation. As it is of continued importance to characterize myocardial tissue non-invasively, it is imperative to have the most reliable and reproducible sequences available for this type of measurement. These results suggest that the 4-echo methods are best suited for optimal T2 and T2* sampling in the mid-ventricular septum. This work presents reliable, high spatial resolution techniques for measuring T2 and T2* and provides reference values for transverse relaxation times in the normal myocardium.

Future work will build on these results by adding the use of newly developed 3rd order shim tools that have been recently applied to SSFP imaging (28). The addition of this technique should improve future results by compensating for susceptibility gradients at the heart-lung interface. The optimal method proposed above will be tested for improved consistency of results utilizing the shim tools.

It would also be of great interest to modify these techniques for use with navigator gated acquisition. Navigator gating would allow for signal averaging in measurements over extended periods of time. Free breathing during navigator acquisition would also be of use when investigating subjects with pathology, as they are presumably less capable of maintaining an extended breath hold.

The high quality of curve fits reported here reflects the accuracy of the measured transverse relaxation values. There is unfortunately no gold standard for *in vivo* cardiac tissue measurement, therefore comparison to other published results in terms of reported means and variance may be the only general measure of accuracy. It is important to further investigate these techniques for use in cardiac research describing the myocardial BOLD effect, perfusion tests, and other aspects of oximetry.

APPENDIX

MATLAB Code

Description: This MATLAB code calculates T2 and T2 maps from multi-echo TSE and TFE source files taken from Philips Achieva series clinical MRI scanners. File handling, ROI selection, SNR, and curve fitting functions are all performed. Co-registration of images is implemented, but is currently commented out for this study as they images were well registered by the Philips console software (v.2.1.3).*

```
%Calc ME Cardiac Signal to Noise Ratio
%Written by Jared Cobb
%VUIIS: Vanderbilt University
%Copyright 2008
%Version: 1/25/08
%Requires: PARMfromPAR_3Ta.m, vuOpenImage.m


clc;clear all;close all;

% COBBJG : START FILE HANDLING

%Open First File
file = vuOpenImage;

%Get filename
filename = file.Parms.filename;
scanNum = file.Parms.acq_nr; %get scan number
%Get Dimensions
[nRows nCols numEcho] = size(file.Data);
%Get scan method, T1TFE or TSE
method = file.Parms.technique;
data = file.Data;

%COBBJG : END FILE HANDLING

% COBBJG : SET / GET ECHO TIMES : CONVERT TO FUNCTION
if strcmp(method,'TSE')
    if numEcho == 4
        echoes = [6 30 54 78]';
        scanEchoes = numEcho;
    elseif numEcho == 8
        echoes = [6 18 30 42 54 66 78 90]';
```

```
        scanEchoes = numEcho;
    end
end
if strcmp(method,'T1TFE')
        echoes = PARMfromPAR_3Ta(filename,31);
        scanEchoes = numEcho;
end
% COBBJG : END GET ECHO TIMES : CONVERT TO FUNCTION

% COBBJG : 2x2E TSE case

if (strcmp('TSE',method) && (numEcho == 2));
    file2 = vuOpenImage;

    %Get filename
    filename2 = file2.Parms.filename;
    scanNum2 = file2.Parms.acq_nr; %get scan number
    %Get Dimensions
    [nRows2 nCols2 numEcho2] = size(file2.Data);
    %Get Echo Times
    echoes = PARMfromPAR_3Ta(filename,31);
    echoes2 = PARMfromPAR_3Ta(filename2,31);
    %Get scan method, T1TFE or TSE
    method2 = file2.Parms.technique;

    if (strcmp(method,method2) == 0)
        'FILE TYPES TO NOT MATCH'
    end

    %reorder data
    data = zeros(nRows,nCols,4);
    data(:,:,1) = file.Data(:,:,1); %20ms
    data(:,:,3) = file.Data(:,:,2); %60ms
    data(:,:,2) = file2.Data(:,:,1); %40ms
    data(:,:,4) = file2.Data(:,:,2); %80ms

    echoes = [echoes(1);echoes2(1);echoes(2);echoes2(2)];
    numEcho = 4;
    scanEchoes = 2;
end
% COBBJG : End 2E TSE case

% COBBJG : Start 3x2E TFE case

if (strcmp('T1TFE',method) && (numEcho == 2));
    file2 = vuOpenImage;
    file3 = vuOpenImage;

 %Get filenames
    filename2 = file2.Parms.filename;
    filename3 = file3.Parms.filename;
    scanNum2 = file2.Parms.acq_nr; %get scan number
    scanNum3 = file3.Parms.acq_nr;
    %Get Dimensions
```

```
    [nRows2 nCols2 numEcho2] = size(file2.Data);
    [nRows3 nCols3 numEcho3] = size(file3.Data);
    %Get Echo Times
    echoes = PARMfromPAR_3Ta(filename,31);
    echoes2 = PARMfromPAR_3Ta(filename2,31);
    echoes3 = PARMfromPAR_3Ta(filename3,31);
    %Get scan method, T1TFE or TSE
    method2 = file2.Parms.technique;
    method3 = file3.Parms.technique;

    if (strcmp(method,method2) == 0)
    'FILE TYPES TO NOT MATCH'
    end

    %reorder data
    data = zeros(nRows,nCols,4);
    data(:,:,1) = file.Data(:,:,1); %2.30ms
    data(:,:,2) = file.Data(:,:,2); %6.91ms
    data(:,:,3) = file2.Data(:,:,2); %11.51ms
    data(:,:,4) = file3.Data(:,:,2); %18.41ms

    scale = zeros(nRows,nCols,3);
    scale(:,:,1) = file.Data(:,:,1); %2.3 ms Data for scaling
    scale(:,:,2) = file2.Data(:,:,1);
    scale(:,:,3) = file3.Data(:,:,1);

    echoes = [echoes(1);echoes(2);echoes2(2);echoes3(2)];
    numEcho = 4;
    scanEchoes = 2;

end

% COBBJG : END 3x2E TFE case

% COBBJG : START SIGNAL MASK

cmap = contrast(data(:,:,1)); %adjust Contrast / Brightness
figure(1)
imagesc(data(:,:,1)); %scales data to colormap and displays pic
zoom(2)
title('Select Cardiac *Signal* ROI')
colormap(cmap)
SignalMask = roipoly; %roipoly selects region of interest

% COBBJG : Implement if not co-registered well.
% if numEcho3 == 2
%    % cmap = contrast(data(:,:,3));
%     figure(2)
%     imagesc(data(:,:,3));
%     zoom(2)
%     colormap(cmap)
%     title('Select second Cardiac Signal ROI')
%     SignalMask2 = roipoly;
%     cmap = contrast(data(:,:,4));
```

```
%     figure(3)
%     imagesc(data(:,:,4));
%     zoom(2)
%     colormap(cmap)
%     title('Select third Cardiac Signal ROI')
%     SignalMask3 = roipoly;
% end
% COBBJG : END co-register

%init ROI 'Signal' and mult by SignalMask from above
Signal = zeros(nRows,nCols,numEcho);
for i = 1:numEcho
    Signal(:,:,i) = SignalMask .* data(:,:,i);
end

% COBBJG : SCALE DATA TO FIRST ECHO
%only occurs in 3x2echo case (I hope!!!!!!!!!!!!!!!!!!!!)
if echoes(4) == 18.41 %must match 4th echo time exactly!
    ScaleMask = zeros(nRows,nCols,3);
    for i = 1:3
    ScaleMask(:,:,i) = SignalMask .* scale(:,:,i); %ROI of all first
echoes
    end
    a = ScaleMask(:,:,1);
    aa = mean(mean(a(a>0)));%mean of 1st scan 2.3ms ROI
    b = ScaleMask(:,:,2);
    bb = mean(mean(b(b>0)));%mean of 2nd scan 2.3ms ROI
    c = ScaleMask(:,:,3);
    cc = mean(mean(c(c>0)));%mean of 3rd scan 2.3ms ROI
    %In theory all these means match.  Scale bb and cc to match aa.
    %scale echoes 3 & 4 to match echo 1 & 2.
    Signal(:,:,3) = Signal(:,:,3) .* aa/bb;
    Signal(:,:,4) = Signal(:,:,4) .* aa/cc;
end
% COBBJG : END SCALE DATA

% COBBJG : END SIGNAL MASK


% COBBJG : START NOISE MASK
figure(2)
imagesc(data(:,:,1)) %scales data to colormap and displays pic
title('Select Cardiac *Noise* ROI')
%colormap(gray)
NoiseMask = roipoly; %roipoly selects region of interest

Noise = zeros(nRows, nCols, numEcho);
for i = 1:numEcho
    Noise(:,:,i) = NoiseMask .* data(:,:,i);
end
% COBBJG : END NOISE MASK

% COBBJG : Calc values for SNR
warning off all
```

```
for i = 1:numEcho
    X = Signal(:,:,i);
    Y = Noise(:,:,i);
    StdSig(i) = std(X(X>0)); %Std of Signal, no zeros included
    MeanSig(i) = mean(X(X>0)); %Mean of Signal
    StdNoise(i) = std(Y(Y>0)); %Std of Noise
    MeanNoise(i) = mean(Y(Y>0)); %Mean of Noise
end
warning on all
% COBBJG : END Calc SNR values

% COBBJG : Start T2/T2* Map for whole image

%create threshold mask
firstImage_m = squeeze(data(:,:,1));
maxValue = max(firstImage_m(:));
mask_m = (firstImage_m > 0.05 * maxValue); % 5% or 10% mask
figure, imagesc(mask_m);  %display mask

warning off all
t2_m = zeros(nRows, nCols);
s0_m = zeros(nRows, nCols);
R_m = zeros(nRows,nCols);
t2lim = 500;  %upper limit based on type o scan.
if (strcmp( 'TSE' , method))
    t2lim = 200;
end
if (strcmp( 'T1TFE' , method))
    t2lim = 100;
end
for row = 1:nRows
    for col = 1:nCols
        if (mask_m(row,col) == 1)
            signal_v = squeeze(data(row, col, :));
            coeff_v = polyfit(echoes, log(signal_v), 1);
            slope = coeff_v(1);
            logS0 = coeff_v(2); % Intercept.
            fit = polyval(coeff_v, echoes);
            R_squared = corrcoef(signal_v, fit);
            t2 = -1 / slope;
            % Force a lower limit on the slope:
            if (t2 > t2lim)
                t2 = t2lim;
            end
            if (t2 < 0)
                t2 = 0;
            end
            %end slope limit
            t2_m(row,col) = t2;
            s0_m(row,col) = exp(logS0);
            R_m(row,col) = R_squared(2);
        end
    end
end
warning on all
```

```
% COBBJG : End T2/T2* Map

% COBBJG : Calc Map values

MapMean_m = SignalMask .* t2_m;
RMean_m = SignalMask .* R_m;
T2Mean = mean(MapMean_m(MapMean_m>0));
T2Std = std(MapMean_m(MapMean_m>0));
RMean = mean(RMean_m(RMean_m > 0));
RStd = std(RMean_m(RMean_m > 0));

% COBBJG : End Calc Map values

% COBBJG : Convert num to str for display
if strcmp( 'TSE' , method)
    TC_name = 'T2';
elseif strcmp( 'T1TFE', method )
    TC_name = 'T2*';
else TC_name = 'Not a T1TFE or TSE Scan!';
end
time_const = -1/slope;
TC = num2str(time_const);
SN = num2str(StdNoise);
MN = num2str(MeanNoise);
MS = num2str(MeanSig);
SS = num2str(StdSig);
%SNR = MeanSig ./ MeanNoise;
SNR = MeanSig / StdNoise;
SNR_text = num2str(SNR);

% COBBJG : END num2str

% COBBJG : Print Relevant Parms to Console
file.Parms.patient
echoes
scanEchoes
T2Mean
T2Std
RMean
RStd
SNR
close all;
figure
imagesc(t2_m);
colorbar;
colormap(gray)
title([TC_name,'Map'])
zoom(2)
xlabel('coordinates (pix)'), ylabel('coordinates (pix)')
%SigMask2 = roipoly;
% COBBJG : END PRINT

% COBBJG : construct data and text to send to Excel
```

```
xlsfile = 'C:/Documents and Settings/cobbjg/My
Documents/MATLAB/Cobb_Cardio_SNR.xlsx';
[NUMERIC,TXT,RAW]=XLSREAD(xlsfile);

%find next row to append in file
[xx,yy] = size(RAW);
zz = xx(1)+1;
xxx = num2str(zz);
xlsrow = strcat('A',xxx);

firstrow = {file.Parms.patient, num2str(scanNum), [num2str(scanEchoes),
' echo ', method]...
    T2Mean, T2Std, RMean, RStd, SNR};

%success = xlswrite(xlsfile, firstrow, 'Raw_Data', xlsrow);
%csvwrite('C:/Documents and Settings/cobbjg/My
Documents/MATLAB/test.csv',firstrow(4:8));

% COBBJG : END Write to Excel
```

REFERENCES

1. Rosamond W, Flegal K, Furie K, et al. *American Heart Association: Heart Disease and Stroke Statistics 2008 Update.* Circulation. 2008; Vol. 117.

2. Haacke EM, Brown RW, Thompson MR, and Venkatesan R. *Magnetic Resonance Imaging: Physical Principles and Sequence Design.* New York : John Wiley and Sons, 1999.

3. Wu YW, Tadamura E, Yamamuro M, et al. *Comparison of contrast-enhanced MRI with (18)F-FDG PET/201Tl SPECT in dysfunctional myocardium: relation to early functional outcome after surgical revascularization in chronic ischemic heart disease.* J Nucl Med. 2007; Vol. 48(7):1096-103.

4. Kühl HP, Lipke CS, Krombach GA, et al. *Assessment of reversible myocardial dysfunction in chronic ischaemic heart disease: comparison of contrast-enhanced cardiovascular magnetic resonance and a combined positron emission tomography-single photon emission computed tomography imaging protocol.* Eur Heart J. 2006; Vol. 27(7): 846-53.

5. Klumpp B, Fenchel M, Hoevelborn T, et al. *Assessment of Myocardial Viability Using Delayed Enhancement Magnetic Resonance Imaging at 3.0 Tesla.* Invest Radiol. 2006; Vol. 41:661-667.

6. Reeder SB, Du YP, Lima JAC, et al. *Advanced Cardiac MR Imaging of Ischemic Heart Disease.* RadioGraphics. 2001; Vol. 21:1047-1074.

7. Cheng A, Karamitsos T, Choudhury R, et al. *Cardiovascular Magnetic Resonance Perfusion Imaging at 3-Tesla for the Detection of Coronary Artery Disease.* JACC, 2007; Vol. (49)25: 2440-2449.

8. Gutberlet M, Noeske R, Schwin K, et al. *Comprehensive Cardiac Magnetic Resonance Imaging at 3.0 Tesla Feasibility and Implications for Clinical Application.* Invest Radiol, 2006; Vol. 41: 154–167.

9. Egred M, Waiter GD, Al-Mohammad A, et al. *Blood oxygen level dependent (BOLD) MRI: A novel technique for the detection of myocardial ischemia.* European Journal of Internal Medicine. 2006; Vol. 17: 551–555.

10. Li D, Dhawale P, Rubin PJ, et al. *Myocardial signal response to dipyridamole and dobutamine: demonstration of the BOLD effect using a*

double-echo gradient-echo sequence. Magn Reson Med. 1996; Vol. (36)1:16-20.

11. Wacker CM, Bock M, Hartlep A, et al. *BOLD-MRI in ten patients with coronary artery disease: evidence for imaging of capillary recruitment in myocardium supplied by the stenotic artery.* MAGMA, 1999; Vol. 8: 48-54.

12. Bauer W, Nadler W, Bock M, et al.*Theory of the BOLD Effect in the Capillary Region: An Analytical Approach for the Determination of T2* in the Capillary Network of Myocardium.* Magnetic Resonance in Medicine. 1990; Vol. 41:51–62.

13. Shea S, Fieno D, Schirf B, et al. *T2-prepared Steady-State Free Precession Blood Oxygen Level–Dependent MR Imaging of Myocardial Perfusion in a Dog Stenosis Model.* Radiology. 2005; Vol. (236)2: 503-509.

14. Simonetti O, Finn J, White R, et al. *"Black blood" T2-weighted inversion-recovery MR imaging of the heart.* Radiology. 1996; Vol. 19(9)1: 49.

15. Greenman R, Shirosky J, Mulkern R, et al. *Double Inversion Black-Blood Fast Spin-Echo Imaging of the Human Heart: A Comparison Between 1.5T and 3.0T.* JMRI. 2003; Vol. 17:648–655.

16. Huang TY, Liu Y, Stemmer A, et al. *T2 Measurement of the Human Myocardium Using a T2-Prepared Transient-State TrueFISP Sequence.* Magnetic Resonance in Medicine. 2007; Vol. 57:960–966.

17. Poon CS, Henkelmann RM. *Practical T2 quantitation for clinical applications.* JMRI. 1992; Vol. 2(5):541-543.

18. Shrager RI, Weiss GH, Spencer RGS. *Optimal time spacings for T2 measurements: monoexponential and biexponential systems.* NMR in Biomedicine. 1998; Vol. 11: 297–305.

19. Bax JJ, van der Wall EE. *Radionuclide techniques for the assessment of myocardial viability and hibernation.* Heart. 2004; Vol. 90: 26-33.

20. Okada S, Katagiri K, Tumazaki T, et al. *Safety of gadolinium contrast agent in hemodialysis patients.* Acta. Radiol. 2001; Vol. (42)3: 399-341.

21. Ersoy H, Rybicki F. *Biochemical Safety Profiles of Gadolinium-Based Extracellular Contrast Agents and Nephrogenic Systemic Fibrosis.* JMRI. 2007; Vol. 26:1190–1197.

22. Strach K, Meyer C, Thomas D, et al. *High-resolution myocardial perfusion imaging at 3 T: comparison to 1.5 T in healthy volunteers.* Eur. Radiol. 2007; Vol. 17: 1829–1835.

23. Di Bella EVR, Parker DL, Sinusas AJ. *On the Dark Rim Artifact in Dynamic Contrast-Enhanced MRI Myocardial Perfusion Studies.* Magnetic Resonance in Medicine. 2005; Vol. 54:1295–1299.

24. Reeder SB, Holmes AA, McVeigh R, et al. *Simultaneous Noninvasive Determination of Regional Myocardial Perfusion and Oxygen Content in Rabbits: Toward Direct Measurement of Myocardial Oxygen Consumption at MR Imaging.* Radiology. 1999; Vol. 212:739-747.

25. Atalay M, Poncelet B, Kantor H, et al. *Cardiac Susceptibility Artifacts Arising From the Heart-Lung Interface.* Magnetic Resonance in Medicine. 2001; Vol. 45:341–345.

26. Reeder SB, Faranesh AZ, Boxerman JL, McVeigh ER. *In vivo measurement of T*2 and field inhomogeneity maps in the human heart at 1.5 T.* Magnetic Resonance in Medicine. 1998; Vol. 39(6):988-98.

27. Foltz W, Al-Kwifi O, Sussman M, et al. *Optimized Spiral Imaging for Measurement of Myocardial T2 Relaxation.* Magnetic Resonance in Medicine. 2003; Vol. 49:1089–1097.

28. Schär M, Kozerke S, Fischer S, et al. *Cardiac SSFP Imaging at 3 Tesla.* Magnetic Resonance in Medicine. 2004; Vol. 51:799–806.

29. Fieno DS, Shea SM, Li Y, et al. *Myocardial perfusion imaging based on the blood oxygen level-dependent effect using T2-prepared steady-state free-precession magnetic resonance imaging.* Circulation. 2004; Vol. 110:1284–1290.

30. Lauzon ML, Mahallati H, Frayne R. *Time-Efficient Breath-Hold Abdominal MRI at 3.0 T.* Am J Roent. 2006; Vol. 187:649–657.

31. Roemer PB, Edelstein WA, Hayes CE, et al. *The NMR phased array.* s.l. : Magn Reson Med. 1990; Vol. 16(2):192-225.

32. Pruessmann K, Weiger M, Scheidegger M, et al. *SENSE: sensitivity encoding for fast MRI.* Magnetic Resonance in Medicine. 1999; Vol. 42(5):952-62.

33. Triantafyllou C, Hoge RD, Krueger G, et al. *Comparison of physiological noise at 1.5 T, 3 T and 7 T and optimization of fMRI acquisition parameters.* 243-250. NeuroImage. 2005; Vol. 26.

34. Henkelman RM. *Measurement of signal intensities in the presence of noise in MR images.* Med Phys. 1985; Vols. Mar-Apr. 12(2):232-3.

35. Rosner, Bernard. *Fundamentals of Biostatistics.* Pacific Grove, CA : Duxbury, 2000; 0-534-37068-3.

36. Does MD, Gore JC. *Complications of nonlinear echo time spacing for measurement of T2.* NMR in Biomedicine. 2000;Vol. 13:1-7.

37. O'Regan D, Callaghan M, Fitzpatrick J, et al. *Cardiac T2* and lipid measurement at 3.0 T-initial experience.* Eur Radiol. 2007; Vol. EPub.

38. Storey P, Thompson AA, Carquiville CL, et al. *R2* imaging of transfusional iron burden at 3T and comparison with 1.5T.* JMRI. 2007; Vol. 25(3):540-7.

39. Selvanayagam J, Jerosch-Herold M, Porto I, et al. *Resting Myocardial Blood Flow Is Impaired in Hibernating Myocardium: A Magnetic Resonance Study of Quantitative Perfusion Assessment.* Circulation. 2005; Vol. 112: 3289-3296.

40. Weiger M, Pruessman K, Boesiger P.*Cardiac real-time imaging using SENSE.* Magnetic Resonance in Medicine. 2000; Vol. 43(2): 177-184.